1

Introduction

1.1 Outline on Wave-Transparent Composites

Wave-transparent composites are a class of functional composites that can pass through electromagnetic waves. On the one hand, wave-transparent composites can provide electromagnetic windows for the transmission and reception of electromagnetic waves to ensure their efficient operation [1]. On the other hand, they can protect the radar antennas, communication, and microwave systems from the harsh external environment such as heavy rain, strong winds, snow, sand, solar radiation, and salt spray [2], ensuring the stability and reliability of electromagnetic wave transmission. With the rapid development of modern electronic information technology as well as the aviation and aerospace industries, the requirements for comprehensive performance of wave-transparent composites are becoming more and more demanding [3].

As far as matrix classification, wave-transparent composites can be divided into ceramic-based and polymer matrix wave-transparent composites [4]. Ceramic-based wave-transparent composites can meet the electrical performance requirements of radar radomes in the centimeter-band electromagnetic wave range. However, for millimeter-band electromagnetic waves (wavelength in the range of 1–10 mm and frequency in the range of 30–300 GHz), ceramic-based wave-transparent composites have disadvantages such as low strength, thick cover walls, and poor wave-transparent performances, which make it difficult to meet the performance requirements of radar radomes for millimeter wave [5, 6].

Polymer matrix wave-transparent composites have the advantages of lightweight, high strength, low dielectric constant (ε) and dielectric loss ($\tan\delta$), and materials/structure/function integration, which have a wide range of promising applications in satellite antennas, aircraft, missiles, 5G ground communication base stations, printed circuit boards, and so on. (Figure 1.1) [7].

This book will describe the wave-transparent mechanism, polymer matrix and reinforced fibers, their two-phase interfaces, molding process, and application prospects of the polymer matrix wave-transparent composites.

Polymer Matrix Wave-Transparent Composites: Materials, Properties, and Applications, First Edition.
Junwei Gu, Yusheng Tang, Jie Kong, and Jing Dang.

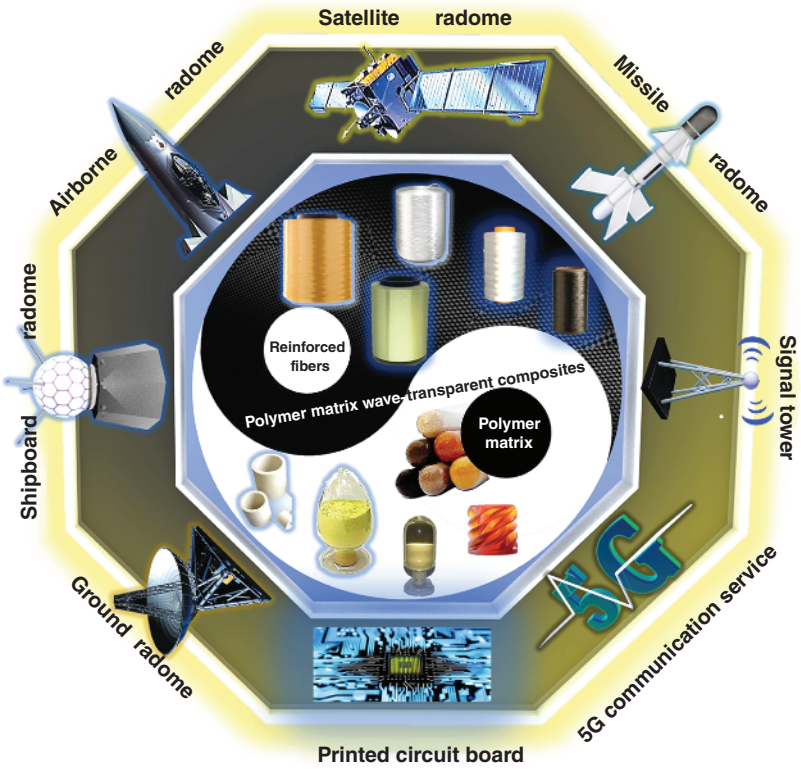

Figure 1.1 Application examples of polymer matrix wave-transparent composites. Source: Polymer matrix wave-transparent composites: A review. Journal of Materials Science & Technology, 2021, 75: 225–251 (Figure 1).

1.2 Composition of Polymer Matrix Wave-Transparent Composites

Polymer matrix wave-transparent composites consist of polymer matrix, reinforced fibers, and two-phase interfaces [8]. Polymers with low ε and $\tan\delta$ values as the matrix fibers with high strength and modulus as reinforced fibers produce advanced polymer-based composites (Figure 1.2) with both mechanical properties and wave-transparent performances *via* hot pressing, vacuum bagging, or resin transfer molding [9].

The heat resistance of polymer matrix determines the thermal stability of the composites in this case, and the fibers mainly serve as reinforcement [10]. Because the dielectric properties of different polymer matrices differ substantially. However, the ε value of reinforced fibers is generally larger than that of polymer matrix. Therefore, the selectively reinforced fibers possess excellent mechanical and thermal properties but also wonderful dielectric properties [11].

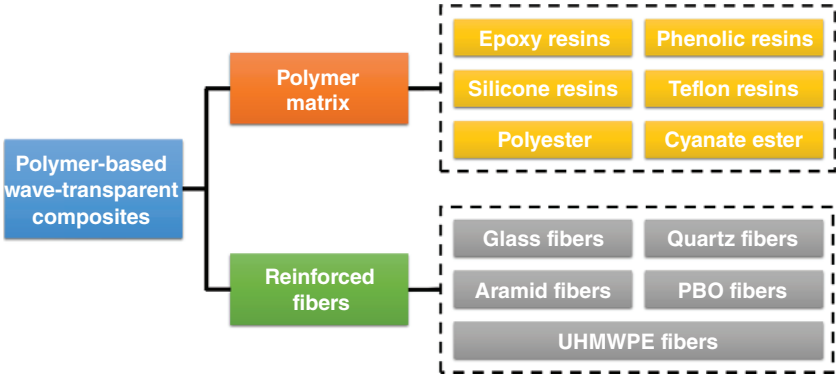

Figure 1.2 Composition of polymer matrix wave-transparent composites (commonly used polymer matrix and reinforced fibers).

1.2.1 Polymer Matrix

Polymers commonly used in wave-transparent composites mainly include epoxy resins [12], phenolic (PF) resins [13], polyimide (PI) resins [14], bismaleimide (BMI) resins [15], silicone resins, polytetrafluoroethylene (PTFE) resins [16], unsaturated polyester (UP) resins [17–19], and cyanate (CE) resins [20]. Table 1.1 shows the main physical and chemical properties of the common polymer matrix.

Epoxy resins have good flowability, low curing shrinkage, and high thermal decomposition temperatures (300–350 °C), but their high ε and $\tan\delta$ values limit their application in high-performance polymer matrix wave-transparent composites [21–23]. PF resins have good heat resistance (long-term service temperature at 250 °C), mechanical properties, and weatherability [24]. However, the ε values of PF resins increase significantly with increasing temperatures [25–27]. PI resins have high heat resistance ($T_g \geq 250$ °C), ε, and $\tan\delta$ values that remain stable over a wide

Table 1.1 Main physical and chemical properties of the common polymer matrix.

Types	Density (g/cm^3)	Flexural strength (MPa)	Flexural modulus (GPa)	ε (10^6 Hz)	$\tan\delta$ (10^6 Hz)
Epoxy	1.30	97	3.8	3.0	0.020
PF	1.30	92	3.5	3.2	0.020
PI	1.36–1.43	170	3.8	3.2	0.007
BMI	1.30	150	3.7	3.0	0.014
Organic silicon	—	85	—	3.0–5.0	0.003–0.050
PTFE	2.20	90	—	2.1–2.3	0.0003–0.0004
UP	1.29	85	3.2	3.0	0.018
CE	1.29	80	2.8	2.8–3.2	0.002–0.008

range of temperatures and frequencies [28]. At the same time, PI resins have excellent mechanical properties, chemical resistance, and dimensional stability [29–31]. However, PI resins are costly and difficult to process [32, 33]. BMI resins are an ideal polymer matrix for advanced composites due to their good heat resistance, excellent mechanical properties, relatively low ε value, resistance to humidity, chemical reagents, and good processability [34, 35]. However, the relatively high tan δ values of BMI resins limit their wider application to a certain extent [36–38]. Silicone resins have excellent heat resistance and stable ε and tan δ values under a wide range of environmental conditions [39–41], but their poor mechanical strength makes them rarely used alone [42–44]. PTFE resins have the lowest ε and tan δ [45, 46] but are not easy to process and have low bonding properties between PTFE matrix and reinforcements [47–49]. UP resins have better mechanical properties than PF resins and have low ε and tan δ values [50–52], which can be cured at room temperature. UP resins have a simple molding process, making them suitable for large-scale or large radome production [53–55]. However, UP resins have a short storage period, relatively low heat deflection temperature, and large curing shrinkage, which makes them unsuitable for the preparation of polymer matrix wave-transparent composites with high dimensional accuracy requirements [56–58].

In comparison, CE resins combine the high-temperature resistance of BMI and PI resins with the good processing properties of epoxy resins [59–61]. The highly symmetrical triazine ring structure and low polarity of the cured CE resins also make them low ε (2.8–3.2) [62–64], good heat resistance, and dimensional stability over a wide temperature and frequency range [65]. The structure and properties of commonly used polymer matrix are described in detail in Chapter 3.

1.2.2 Reinforced Fibers

Reinforced fibers for polymer matrix wave-transparent composites mainly include glass fibers [66, 67], quartz fibers [68], Kevlar fibers [69, 70], ultra-high-molecular-weight polyethylene (UHMWPE) fibers [71, 72], and poly(*p*-phenylene-2,6-benzobisoxazole) (PBO) fibers [73, 74]. Their main physical and chemical properties are shown in Table 1.2.

Table 1.2 Main physical and chemical properties of common reinforced fibers.

Properties Types	Density (g cm^{-3})	Tensile strength (GPa)	Modulus (GPa)	ε (10^6 Hz)	tan δ (10^6 Hz)
E-glass fibers	2.54	3.75	72	6.13	0.0038
S-glass fibers	2.49	4.00	85	5.21	0.0068
D-glass fibers	2.6	2.40	52	4.00	0.0025
Quartz fibers	2.20	1.70	72	3.78	0.0002
Kevlar49 fibers	1.45	3.45	137	3.85	0.0010
UHMWPE fibers	0.97	5.01	193	2.25	0.0002
PBO fibers	1.56	5.80	280	3.00	0.0010

Figure 1.3 Application examples of D-glass fibers reinforced polymer matrix wave-transparent composites: MIRAGE 2000 (France, a); GRIPEN JAS 39 – Credit: Thierry ducros/Airliners.net (Sweden, b); HAWK 200 – Credit: Ben Stacey/Flickr (United Kingdom, c); HARRIER – Credit: Weimeng/Air Team Images (United Kingdom, d). HARRIER GR.9 – Credit: Titan Miller/Airliners.net. Source: (b) Ben Stacey/Flickr.

Glass fibers are the most commonly used inorganic reinforced fibers for wave-transparent composites. The earliest glass fibers used were E-glass fibers [75, 76]. Then, high-strength glass fibers (S-glass fibers) [77–79] and high-silica glass fibers (D-glass fibers) [80, 81] were developed to meet the special needs of aviation, aerospace, military, and other high-tech fields. Compared to E-glass and S-glass fibers, D-glass fibers have relatively lower ε and $\tan\delta$, which has been used in the radomes of MIRAGE 2000 (France), GRIPEN JAS 39 (Sweden), HAWK 200 (United Kingdom), and HARRIER (United Kingdom) (Figure 1.3) [82, 83].

However, with the rapid development of information technology, electronic components receive and transmit electromagnetic waves at increasingly high frequencies [84]. The high content of alkali metal oxides in glass fibers and the strong signal hysteresis and attenuation produced during electromagnetic wave transmission limit their application in high-frequency and high-precision wave-transparent composites [85]. Quartz fibers contain only a single component of silicon dioxide (SiO_2) with purity of over 99.9% and have excellent high-temperature resistance, electrical insulation properties and ablation resistance, low ε and $\tan\delta$ values, and so on [86, 87], which have been one of the most commonly used reinforced fibers in wave-transparent composites in the military and civilian sectors. However, quartz fibers have disadvantages such as high density, poor mechanical properties, and large ε values [88].

With the increasing demand for comprehensive performances of polymer matrix wave-transparent composites in terms of weight reduction, wave-transparency, and loading, researchers have carried out relevant research on organic reinforced fibers such as Kevlar fibers [89], UHMWPE fibers [90] and PBO fibers [91, 92]. Kevlar fibers, with low density, high specific strength, and specific modulus, are one of the most commonly used organic reinforced fibers in polymer matrix

wave-transparent composites [93–95]. However, the high moisture absorption of Kevlar fibers is susceptible to moisture swelling and cracking, resulting in the degradation of wave-transparent performances and mechanical properties [96]. UHMWPE fibers, also known as high-strength, high-modulus polyethylene fibers, have a relative molecular mass of over 1 million, which is beneficial to outstanding impact resistance, cut resistance, chemical resistance and UV resistance, excellent low-temperature resistance, and low ε and $\tan\delta$ values [97, 98]. However, as the macromolecular chains of UHMWPE fibers are connected by a highly symmetrical methylene structure, the intermolecular Van der Waals forces are weak, making their T_g and melting point low, resulting in their high-temperature resistance and poor creep resistance [99].

Moreover, the surface of UHMWPE fibers does not contain polar groups, resulting in low surface energy, which creates poor bond strength between the UHMWPE fibers and polymer matrix [100, 101]. As a super fiber of the twenty-first century, the large number of rigid aromatic and oxazole rings in the PBO fiber molecular chain and a highly ordered crystal structure give PBO fibers excellent mechanical properties, heat resistance, chemical stability, and low ε (3.0) and $\tan\delta$ (0.001) values, which are of wide interest in the field of airborne/starborne radar radomes. Furthermore, PBO fibers have higher tensile strength, lower density, and ε values than those of inorganic reinforced fibers such as quartz [102]. Compared to those of other organic fibers, PBO fibers have about twice the strength and modulus of para-Kevlar fibers, and the thermal decomposition temperature of PBO fibers in the air is about 650 °C, which is approximately 100 °C higher than that of Kevlar fibers and much better than that of UHMWPE fibers (300 °C) [103]. As a result, PBO fibers have received a lot of attention as potential reinforcements for light weight/loading/wave-transparent integrated wave-transparent composites [104]. However, PBO fibers still have disadvantages of high cost, smooth and inert

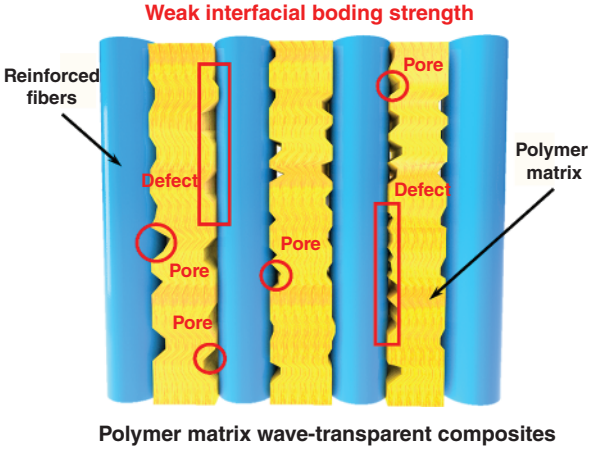

Figure 1.4 Schematic diagram of the two-phase interface for polymer matrix wave-transparent composites.

surfaces, and so on [105–107]. The structure and properties of these commonly used reinforced fibers are described in detail in Chapter 4.

In addition, the microscopic phase interface links the polymer matrix and reinforced fibers [108]. Defects are likely to arise at the poor two-phase interface (Figure 1.4), which would affect the overall performance (especially the interlaminar shear strength, ILSS) of the polymer-matrix wave-transparent composites [109, 110].

Therefore, how to effectively enhance the interfacial compatibility between polymer matrix and reinforced fibers has become a hot and difficult issue in this field [111]. Chapter 5 provides a detailed description of the two-phase interface inner polymer matrix wave-transparent composites and their optimal control strategies.

1.3 Factors Influencing the Wave-Transparent Performances of Polymer Matrix Wave-Transparent Composites

Polymer matrix wave-transparent composites are mainly used for electromagnetic windows and radomes in the fields of aviation/aerospace, 5G communication, and electronic information [112]. In order to ensure that all types of radar and antenna systems remain in stable operating conditions under harsh external environments, polymer matrix wave-transparent composites are required to have excellent wave-transparent performances (low ε and $\tan\delta$ values) [113].

The main factors affecting the wave-transparent performances of polymer matrix composites are divided into internal factors (intrinsic ε and $\tan\delta$) and external factors (thickness and electromagnetic wave frequency) [114, 115]. In general, the lower the molecular polarization rate and the density of polarized molecules of polymer matrix and reinforced fibers, the lower the ε and $\tan\delta$ of polymer matrix wave-transparent composites, the less energy is reflected and lost during the transmission of electromagnetic waves, and the correspondingly higher the wave-transparent rate [116]. In addition, polymer matrix wave-transparent composites are typically multiphase systems, and the interface between polymer matrix and reinforced fibers is prone to interfacial polarization, increasing the ε and $\tan\delta$ values, which is not conducive to improving the wave-transparent performance [117].

In addition, the thickness of polymer-based wave-transparent composites also affects their wave-transparent performances [118]. When the frequency of the electromagnetic wave is constant, the thickness of the wave-transparent composites increases, resulting in a tendency for the wave-transparent rate to decrease and then increase (Figure 1.5) [119]. This is mainly due to the reflection and loss (both absorption and interference shifts) that occur on the surface and inside the wave-transparent composites as the electromagnetic waves pass through [120, 121]. When the thickness approaches an odd multiple ($d = n\lambda/4$, $n = 1, 3, 5$, etc.) of its quarter wavelength ($\lambda/4$, Eq. 1.1), electromagnetic waves cause strong interference cancellation in the wave-transparent composites. This leads to an attenuation of the

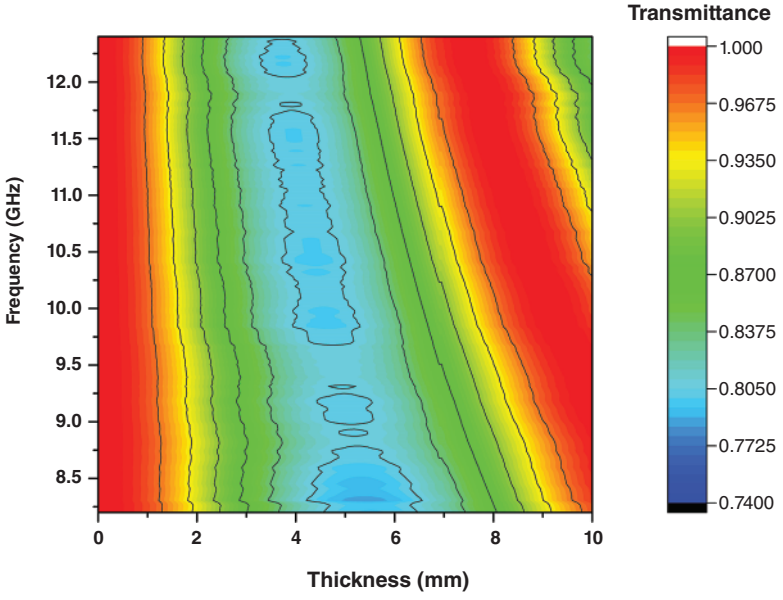

Figure 1.5 Schematic representation of wave transmission versus material thickness for polymer matrix wave-transparent composites.

electromagnetic wave energy and a significant reduction of the transmitted waves, resulting in the reduction of the wave transmission [122–124]. When the thickness is close to an even multiple ($d = n\lambda/4$, $n = 2, 4, 6$, etc.) of $\lambda/4$, the electromagnetic waves reflect less at the incident interface and can enter the interior almost unharmed, with the high wave transmission rate [125, 126].

$$n\lambda/4 = nc/4f_{\mathrm{m}} * (u_{\mathrm{r}} * \varepsilon_{\mathrm{r}})^{1/2} \tag{1.1}$$

where λ represents the wavelength of the incident waves; c represents the speed of light; f_{m} represents the frequency of the incident waves; u_{r} represents the magnetic permeability of the medium; and ε_{r} represents the dielectric constant of the medium.

1.4 Property Requirements for Polymer Matrix Wave-Transparent Composites

1.4.1 Wave-Transparent Performances

The ε and $\tan\delta$ values of polymer matrix wave-transparent composites are among the most important parameters affecting the wave-transparent performances [127]. In practice, the transmission rate of electromagnetic waves is usually required to exceed 70% in the broad frequency range (0.3–300 GHz), which usually requires the corresponding ε of polymer matrix wave-transparent composites to be stable in the range of 1–4 and $\tan\delta$ in the range of 10^{-2}–10^{-3}. Meanwhile, the ε and $\tan\delta$ are required to remain constant in the broad frequency and temperature range (0–220 °C) [128, 129].

1.4.2 Mechanical Properties

As structural loading materials, polymer matrix wave-transparent composites must have a certain degree of stiffness and strength to ensure the stability and reliability of the antenna system in various complex operating environments [130]. The tensile strength of polymer matrix wave-transparent composites for high-performance radomes is generally not less than 400 MPa. The compressive strength is more than 350 MPa to ensure the integrity of the antenna system under aerodynamic loads and impact of foreign objects, thus ensuring the normal operation of the electronic components inside the radomes [131–133].

1.4.3 Heat Resistant Properties

When the vehicle is flying at ultra-high speed in the atmosphere, the surface temperature of vehicle rises sharply with the increase in Mach number due to the heating of the high-temperature compressed gas between the excitation wave and the body and the strong friction between the surface of the body and the air (usually when the Mach number is 2, the surface temperature of the vehicle is about 150 °C; while when the Mach number increases to 3, the surface temperature rises sharply to about 350 °C, even exceeding the strength limit temperature of aluminum alloy) [134], therefore, when polymer matrix wave-transparent composites are used as radomes for aircraft, they should have excellent heat resistance (pyrolysis temperature greater than 300 °C) to overcome the high thermal stresses of external aerodynamic heating and to avoid deformation or even cracks under rapid temperature change [135, 136].

1.4.4 Environmental Resistance Properties

As protective materials for radar antenna systems, polymer matrix wave-transparent composites are subject to surface aging, polymer matrix degradation, and interfacial debonding between the polymer matrix and reinforced fibers during long-term service, which would seriously affect their service stability and reliability [137, 138]. Therefore, polymer matrix wave-transparent composites are required to have excellent environmental aging resistances. Current research revealed that environmental factors (humidity, heat, high and low-temperature alternation, and light) had a significant effect on the mechanical and dielectric properties of glass fiber-reinforced epoxy resin wave-transparent composites. When the relative humidity increased from 25% to 85%, the ε and $\tan\delta$ increased by 10% and 18.6%, respectively. In addition, the mechanical properties were strongly influenced by the hygrothermal conditions. The retention of tensile and flexural strengths after boiling for 200 hours was about 90%, but the retention of ILSS was only 61% [139].

References

1 Hamid, S., Heberling, D., Junghahnel, M. et al. (2022). Development of a millimeter-wave transparent antenna inside a headlamp for automotive radar application. *International Journal of Microwave and Wireless Technologies* 14 (6): 677–688.

2 Wang, M., Li, J., Shao, B., and Xiang, P. (2022). Progress of low dielectric property modified in 5G. *Plastics* 51 (1): 117–120.

3 Zhao, Y. and Pan, L. (2021). Research progress of aerospace advanced polymer matrix composites and manufacturing technology. *Aerospace Materials & Technology* 51 (4): 29–36.

4 Cao, W., Yang, X., and Zhang, O. (2020). Development and prospect of high performance polymer composites in China. *Engineering Sciences* 22 (5): 112–120.

5 Bin, F., Sun, W., and Liu, Y. (2021). Design technique of millimeter wave transparent window. *Journal of Microwaves* 37 (4): 21–24. 9.

6 Kamutzki, F., Schneider, S., Barowski, J. et al. (2021). Silicate dielectric ceramics for millimetre wave applications. *Joural of the European Ceramic Society* 41 (7): 3879–3894.

7 Gopinathapanicker, J.C., Inamdar, A., Anand, A. et al. (2020). Radar transparent, impact-resistant, and high-temperature capable radome composites using polyetherimide-toughened cyanate ester resins for high-speed aircrafts through resin film infusion. *Industrial & Engineering Chemistry Research* 59 (16): 7502–7511.

8 Li, X., He, R., and Liu, H. (2022). Progress in low dielectric polymer materials. *Journal of Functional Materials* 53 (4): 597–606.

9 Hu, Z.D., Liu, X.Q., Ren, T.L. et al. (2022). Research progress of low dielectric constant polymer materials. *Journal of Polymer Engineering* 42 (8): 677–687.

10 Yang, X.J., Li, B., Li, D. et al. (2019). High-temperature properties and interface evolution of silicon nitride fiber reinforced silica matrix wave-transparent composite materials. *Journal of the European Ceramic Society* 39 (2-3): 240–248.

11 Wu, S.H., Li, C.C., Yu, Z.H. et al. (2020). Nondestructive strategy to effectively enhance the interfacial adhesion of PBO/epoxy composites. *ACS Applied Materials & Interfaces* 12 (40): 45383–45393.

12 Li, P., Du, R., Liu, Y., and Zhao, G. (2021). Preparation of epoxy resin/quartz fiber wave-transparent composites. *Engineering Plastics Application* 49 (2): 29–33. 9.

13 Zhao, Y., Xu, R., Xiao, Y. et al. (2022). Mechanical performances of phenolic modified epoxy resins at room and high temperatures. *Coatings* 12 (5): 643.

14 Wang, S., Jiang, S., Han, X. et al. (2021). Research progress on high-performance polyimide resins and their composites. *Journal of Functional Polymers* 34 (6): 570–585.

15 Zhang, Z.W., Zhou, Y.J., Cai, L.F. et al. (2022). Synthesis of eugenol-functionalized polyhedral oligomer silsesquioxane for low-k bismaleimide resin combined with excellent mechanical and thermal properties as well as its composite reinforced by silicon fiber. *Chemical Engineering Journal* 439: 135740.

16 Zhang, Y., Wang, R., Zhang, X., and Guo, S. (2022). Ingenious sandwich-like adhesive films and controllable introduction of fluorine-containing groups toward strong adhesive strength and low dielectric characteristics. *Industrial & Engineering Chemistry Research* 61 (39): 14494–14507.

17 Gao, Y., Romero, P., Zhang, H.L. et al. (2019). Unsaturated polyester resin concrete: a review. *Construction and Building Materials* 228: 116709.

18 Poorabdollah, M. and Kamran, A. (2019). Optimising cure cycle of unsaturated polyester nanocomposites using directed grid search method. *Polymers and Polymer Composites* 27 (5): 253–261.

19 Zong, D., Zhang, Y., Chen, J., and Liu, Y. (2021). Influencing factors in low temperature curing shrinkage of unsaturated polyester resin. *Journal of Materials Science and Engineering* 39 (1): 77–81. 100.

20 Llevot, A., Grau, E., Carlotti, S. et al. (2016). From lignin-derived aromatic compounds to novel biobased polymers. *Macromolecular Rapid Communications* 37 (1): 9–28.

21 Luo, X., Liu, S., and Zhao, J. (2021). Research progress in low dielectric loss epoxy resin composites. *China Plastics* 35 (3): 130–138.

22 Mi, X.Q., Liang, N., Xu, H.F. et al. (2022). Toughness and its mechanisms in epoxy resins. *Progress in Materials Science* 130: 100977.

23 Muller-Pabel, M., Agudo, J.A.R., and Gude, M. (2022). Measuring and understanding cure-dependent viscoelastic properties of epoxy resin: a review. *Polymer Testing* 114: 107701.

24 Wang, Y.N., Liu, J., and Han, X. (2018). Research progress and application of phenolic resin-based prepreg. *New Chemical Materials* 46 (7): 269–272.

25 Cao, Y., Li, X., Li, Y. et al. (2020). Properties of high silica glass fiber/phenolic composites by soft molding. *Aerospace Materials & Technology* 50 (2): 99–102.

26 Guo, Y., Hu, L., and Zhou, Y. (2018). Research progress on phenolic resin modified with silicon. *New Chemical Materials* 46 (10): 5–9.

27 Tong, Y., Li, L., Liu, H. et al. (2019). Research progress on high temperature resistant resins. *Thermosetting Resin* 34 (3): 51–54. 60.

28 Xue, S., Lei, X., Lian, R. et al. (2021). Progress of high-performance thermosetting polyimide resins. *Polymer Materials Science & Engineering* 37 (5): 149–162.

29 Li, X.T., Liu, T., Jiao, Y.Z. et al. (2019). Novel high-performance poly(benzoxazole-co-imide) resins with low dielectric constants and superior thermal stabilities derived from thermal rearrangement of ortho-hydroxy polyimide oligomers. *Chemical Engineering Journal* 359: 641–651.

30 Sun, G., Zhang, X., Wu, D., and Hou, L. (2021). Research progress in high-performance polyimide composites. *China Plastics* 35 (9): 147–155.

31 Wu, T., Fang, Y.T., Dong, J. et al. (2021). Synthesis and properties of polyimide resin containing acetylene and benzoxazine double crosslinking moieties. *Chemical Journal of Chinese Universities* 42 (6): 1978–1986.

32 Huang, X., Peng, X., Liu, R. et al. (2021). Theprogress of low dielectric constant modified polyimide materials. *Journal of Functional Materials* 52 (5): 5018–5024.

33 Iredale, R.J., Ward, C., and Hamerton, I. (2017). Modern advances in bismaleimide resin technology: a 21st century perspective on the chemistry of addition polyimides. *Progress in Polymer Science* 69: 1–21.

34 Ma, X., Guo, Y., and Zhang, Y. (2019). Research progress of ablative resins for RTM. *Thermosetting Resin* 34 (1): 66–70.

35 Mao, Y.M., Yao, Z.J., Zhou, J.T. et al. (2020). Fabrication and investigations on BMI/OMMT nanocomposites with superior high-temperature wave-transparent performance. *Journal of Materials Science: Materials in Electronics* 31 (18): 16073–16086.

36 Liu, B., Yang, L., Li, F. et al. (2020). Research on properties of bismaleimide/T700 carbon fiber resin composite. *Engineering Plastics Application* 48 (11): 117–120.

37 Wen, Y., Li, B., He, Y. et al. (2018). Study on the curing reaction kinetics of modified bismaleimide resin. *China Plastics Industry* 46 (12): 22–26.

38 Zhang, Z.W., Tian, D., Niu, Z.Q. et al. (2021). Enhanced toughness and lowered dielectric loss of reactive POSS modified bismaleimide resin as well as the silica fiber reinforced composites. *Polymer Composites* 42 (12): 6900–6911.

39 Guan, S.J., Wu, F., Wu, Q. et al. (2021). Modification of silicone resins by Si-N cross-dehydrocoupling with perfect thermal stability and mechanical performance. *New Journal of Chemistry* 45 (35): 15892–15900.

40 Liu, Y., Chen, Z.X., Qin, Y.S. et al. (2020). Silicone resin-based composite materials for high thermal stability and thermal conductivity. *Journal of Electronic Materials* 49 (7): 4379–4384.

41 Zheng, J.Y., Cai, Y.Q., Hu, Y. et al. (2022). Bio-based epoxy functionalized MQ silicone resins: from synthesis to toughened epoxy composites with good mechanical properties, thermal resistance and transparency. *Polymer Chemistry* 13 (37): 5325–5336.

42 Huang, C., Zheng, C., Zheng, G. et al. (2020). Preparation and application of silicone resin based wear-resistant composite fiber material. *New Chemical Materials* 48 (1): 245–249.

43 Ling, Y.Q., Zhang, X.Q., Yan, L.W. et al. (2022). Silicone-grafted epoxy/carbon fiber composites with superior mechanical/ablation performance. *Materials Chemistry and Physics* 275.

44 Zhu, Q.Q., Wang, Z.H., Zeng, H. et al. (2021). Effects of graphene on various properties and applications of silicone rubber and silicone resin. *Composites Part A: Applied Science and Manufacturing* 142: 106240.

45 Pan, C., Kou, K., Jia, Q. et al. (2017). Improved thermal conductivity and dielectric properties of hBN/PTFE composites via surface treatment by silane coupling agent. *Composites Part B: Engineering* 111: 83–90.

46 Zheng, L., Zhou, J., Shen, J. et al. (2019). Effects on the thermal expansion coefficient and dielectric properties of CLST/PTFE filled with modified glass fiber as microwave material. *Chinese Chemical Letters* 30 (5): 1111–1114.

47 Jiang, Z. and Yuan, Y. (2018). Effects of particle size distribution of silica on properties of PTFE/SiO2 composites. *Materials Research Express* 5 (6): 066306.

48 Li, X. and Ge, Z. (2020). A review on PTFE composites filled with inorganic materials. *China Plastics* 34 (1): 92–101.

49 Wang, L., Jin, X., Wu, C., and Zhang, L. (2021). Effect of glass fiber on properties of PTFE/SiO_2 composite substrate. *Engineering Plastics Application* 49 (1): 130–134.

50 Chen, X., Li, Y., Chen, J. et al. (2018). Research progress in unsaturated polyester resin modified by inorganic nanoparticles. *China Plastics* 32 (3): 1–5.

51 Liu, C. and Zhou, Y. (2020). Progress in oil-based unsaturated polyester resins. *Chemistry and Industry of Forest Products* 40 (6): 107–117.

52 Sapuan, S.M., Aulia, H.S., Ilyas, R.A. et al. (2020). Mechanical properties of longitudinal basalt/woven-glass-fiber-reinforced unsaturated polyester-resin hybrid composites. *Polymers* 12 (10): 2211.

53 Farsane, M., Lhasnaoui, S., Anouar, A. et al. (2022). A review of measureing the gelation time in unstrated polyester resins. *Materials and Technologies* 56 (3): 323–329.

54 Moujdin, I.A., Totah, H.S., Abulkhair, H.A. et al. (2022). Development of low shrinkage curing techniques for unsaturated polyester and vinyl ester reinforced composites. *Materials* 15 (9): 2972.

55 Wu, S., Liu, J., Shao, C. et al. (2020). Application of UPR in solid propellant inhibitor. *New Chemical Materials* 48 (3): 6–8.

56 Chen, M.Z., Wang, X.J., Zhang, J., and Zhu, J.J. (2022). Synergistic action of initiator and accelerator on curing thermodynamics and kinetics of chopped carbon fiber-reinforced low-density unsaturated polyester resin with rapid polymerization. *Journal of Thermal Analysis and Calorimetry* 147: 14195–14199.

57 Delaite, C., Bistac, S., Dreyer, E., and Schuller, A.S. (2020). Influence of initiator on the curing of unsaturated polyester resin at 100°C. *Polymer International* 69 (11): 1089–1096.

58 Han, D., Cao, H., Chen, J. et al. (2018). Study on the UV-curing behavior of unsaturated polyester resin by in-situ Fourier transform infrared. *Thermosetting Resin* 33 (5): 9–14.

59 Chen, S., Yuan, L., Wang, Z.H. et al. (2019). Self-constructed nanodomain structure in thermosetting blend based on the dynamic reactions of cyanate ester and epoxy resins and its related property. *Composites Part B: Engineering* 177: 107438.

60 Jayalakshmi, C.G., Salunke, A.D., Joshi, M. et al. (2022). Cyanate ester- epoxy blends toward microwave transparent polymer composites through resin film infusion for wideband electromagnetic applications. *Polymer-Plastics Technology and Materials* 61 (2): 145–160.

61 Zhang, X., Wang, F., Zhu, Y., and Qi, H. (2021). Preparation and property of modified cyanate ester resin. *New Chemical Materials* 49 (6): 164–170.

62 Li, C.P. and Chuang, C.M. (2021). Thermal and dielectric properties of cyanate ester cured main chain rigid-rod epoxy resin. *Polymers* 13 (17): 2917.

63 Qiao, H., Bao, J., Zhong, X. et al. (2019). Modification and thermal analysis for curing properties of cyanate-ester resin. *Journal of Aeronautical Materials* 39 (6): 63–72.

64 Wang, Z.C., Li, R.J., Qin, Q.R. et al. (2022). Curing kinetics and mechanical properties of cyanate ester/hyperbranched benzoxazine copolymers. *Polymers for Advanced Technologies* 33 (5): 1606–1616.

65 Zhou, Y.J., Zhang, Z.W., Wang, P.R., and Ma, X.Y. (2022). High-performance and low-dielectric cyanate ester resin optimized by regulating the structure of linear polyhydroxy ether modifier. *Composites Part A: Applied Science and Manufacturing* 162: 107136.

66 Lu, Y., Dang, Z., and Cao, F. (2021). Preparation and flame retardancy of glass fiber reinforced polypropylene composite. *Plastics* 50 (2): 15–18.

67 Praneeth, A., Kumar, K., Pramod, R., and Kumar, G.B.V. (2019). Investigation of mechanical properties of glass fibre reinforced honeycomb panels. In: *International Conference on advances in Materials and Manufacturing Applications*.

68 Zhang, Y., Zhang, L., Tao, Y. et al. (2018). Effects of laser ablation on electric properties of quartz fiber/cyanate resin wave-transmitting composite. *Acta Materiae Compositae Sinica* 35 (11): 3001–3007.

69 Dai, Y., Meng, C.B., Cheng, Z. et al. (2019). Nondestructive modification of aramid fiber based on selective reaction of external cross-linker to improve interfacial shear strength and compressive strength. *Composites Part A: Applied Science and Manufacturing* 119: 217–224.

70 Zhao, Y., Li, X., Shen, J.N. et al. (2020). The potential of Kevlar aramid nanofiber composite membranes. *Journal of Materials Chemistry A* 8 (16): 7548–7568.

71 Chen, M., Lin, H., Yang, C., and Li, L. (2022). Research progress on modification of ultra high molecular weight polyethylene (UHMWPE) fiber. *Applied Chemical Industry* 51 (2): 520–524.

72 Chhetri, S. and Bougherara, H. (2021). A comprehensive review on surface modification of UHMWPE fiber and interfacial properties. *Composites Part A: Applied Science and Manufacturing* 140: 106146.

73 Chin, J., Forster, A., Clerici, C. et al. (2007). Temperature and humidity aging of poly (p-phenylene-2,6-benzobisoxazole) fibers: chemical and physical characterization. *Polymer Degradation and Stability* 92 (7): 1234–1246.

74 Kuroki, T., Tanaka, Y., Hokudoh, T., and Yabuki, K. (1997). Heat resistance properties of poly(p-phenylene-2,6-benzobisoxazole) fiber. *Journal of Applied Polymer Science* 65 (5): 1031–1036.

75 Al-Furjan, M.S.H., Shan, L., Shen, X. et al. (2022). A review on fabrication techniques and tensile properties of glass, carbon, and Kevlar fiber reinforced polymer composites. *Journal of Materials Research and Technology* 19: 2930–2959.

76 Naito, K. (2022). Static and fatigue tensile properties of carbon/glass hybrid fiber-reinforced epoxy composites. *Scientific Reports* 12 (1): 6298.

77 Cho, K., Wang, G.N., Raju, R. et al. (2019). Influence of surface treatment on the interfacial and mechanical properties of short s-glass fiber reinforced dental composites. *ACS Applied Materials & Interfaces* 11 (35): 32328–32338.

78 Xiong, Q., Liu, Z., Chen, W., and Yan, C. (2021). Study on the performance of glass fiber used for superconducting magnet insulation before and after vacuum heat treatment process. *Chinese Journal of Vacuum Science and Technology* 41 (8): 756–760.

79 Yeon, J., Chowdhury, S.C., and Gillespie, J.W. (2022). Mechanical properties and damage analysis of S-glass: a reactive molecular dynamics study. *Composites Part B: Engineering* 234: 109706.

80 Chen, C., Zhu, Q.O., Wang, H.P. et al. (2022). Excellent mechanical properties of the silicate glasses modified by CeO_2 and TiO_2: a new choice for high-strength and high-modulus glass fibers. *Silicon* 14 (8): 4301–4308.

81 Liu, K., Chen, B., Dai, J., and Zhu, S. (2010). Effect of environment factors on properties of glass fiber reinforced epoxy resin wave-transparent composites. *The Journal of Engineering Plastics Application* 38 (10): 64–67.

82 Feng, Z., Li, J., Zuo, X. et al. (2021). Progress of composite materials for aerospace applications. *Aerospace Materials & Technology* 51 (4): 23–28.

83 Zhang, S., Luo, L., Ding, L. et al. (2021). Effect of acid leaching on structure and properties of high silica glass fibers. *Journal of the Chinese Ceramic Society* 49 (8): 1543–1549.

84 Kong, L.M., Zheng, W., Wang, X.B. et al. (2021). Effects of layering types and fiber off-axis angle on the mechanical properties of s-glass-fiber-reinforced composites. *Mechanics of Composite Materials* 57 (4): 551–562.

85 Zurowski, W., Zepchlo, J., Krzyzak, A. et al. (2022). Effect of the quartz powder on the performance of the two layers glass fiber reinforced polymer composite with emulsion binder. *Composite Structures* 298: 116024.

86 Cui, G., Cheng, Y., Liu, C. et al. (2020). Massive growth of graphene quartz fiber as a multifunctional electrode. *ACS Nano* 14 (5): 5938–5945.

87 Kong, G., Wang, K., Yu, Q. et al. (2022). Properties of aerogel modified quartz fiber reinforced silicone wave-transparent composites. *Acta Armamentarii* 43 (2): 442–450.

88 Wang, X., Yang, S., Li, G. et al. (2021). Research on mechanical properties of carbon/quartz hybrid fiber composite. *China Plastics Industry* 49 (7): 87–90.

89 Liu, Y.L., Ye, L., Shu, Y., and Zhao, X.W. (2018). In situ preparation of intrinsic flame retardant urea formaldehyde/aramid fiber composite foam: structure, property and reinforcing mechanism. *Composites Part A: Applied Science and Manufacturing* 115: 274–282.

90 Li, L., Han, L., Wang, S. et al. (2022). Research progress on surface modification and interfacial properties of UHMWPE fiber. *Journal of Functional Materials* 53 (4): 012016.

91 Liu, Z., Fan, X.L., Zhang, J.L. et al. (2021). Improving the comprehensive properties of PBO fibres/cyanate ester composites using a hyperbranched fluorine and epoxy containing PBO precursor. *Composites Part A: Applied Science and Manufacturing* 150: 106596.

92 Ni, X.Y., Feng, H., Li, L.H. et al. (2021). A novel poly(p-phenylene benzobisoxazole) (PBO)-based three-phase silk-cocoon network structure nanocomposites with enhanced dielectric properties. *Journal of Materials Science: Materials in Electronics* 32 (6): 7574–7586.

93 Lv, J.W., Yin, J.Y., Qin, Y.T. et al. (2021). Post-construction of weaving structure in aramid fiber towards improvements of its transverse properties. *Composites Science and Technology* 208: 108780.

94 Priyanka, P., Dixit, A., and Mali, H.S. (2019). High strength Kevlar fiber reinforced advanced textile composites. *Iranian Polymer Journal* 28 (7): 621–638.

95 Zhang, B., Jia, L.H., Tian, M. et al. (2021). Surface and interface modification of aramid fiber and its reinforcement for polymer composites: a review. *European Polymer Journal* 147: 110352.

96 Sharma, P., Mali, H.S., and Dixit, A. (2021). Mechanical behavior and fracture toughness characterization of high strength fiber reinforced polymer textile composites. *Iranian Polymer Journal* 30 (2): 193–233.

97 Dayyoub, T., Maksimkin, A.V., Senatov, F.S. et al. (2020). Treating UHMWPE surface for enhancing the adhesion properties by cellulose grafting. *International Journal of Adhesion and Adhesives* 98: 102535.

98 Wang, H.Q., Quan, J.Y., Wang, X.W. et al. (2021). The effect of shrinkage on the structure and properties of ultra-high molecular weight polyethylene fibers with different concentration. *Journal of Applied Polymer Science* 138 (15): e50198.

99 Wang, X., Zhang, Y., Sun, Y. et al. (2020). Research progress of ultra high molecular weight polyethylene. *Chemical Industry and Engineering Progress* 39 (9): 3403–3420.

100 Shang, Q., Zhao, H., Zhao, N. et al. (2020). Research progress on surface modification of ultra-high molecular weight polyethylene fiber. *Polymer Bulletin* 4: 22–29.

101 Tang, L., Guo, Z., Lei, S. et al. (2019). Advances in ultra-high molecular weight polyethylene for the production of fiber. *Petrochemical Technology* 48 (8): 864–870.

102 Song, B., Liu, Z.D., Chen, L. et al. (2022). Enhancing interfacial adhesion and mechanical performance of PBO fibers composites through mussel-inspired molecular regulation of interphase structure. *Polymer Composites* 43 (1): 454–466.

103 Naveen, J., Jayakrishna, K., Sultan, M.T.B., and Amir, S.M.M. (2020). Ballistic performance of natural fiber based soft and hard body armour: a mini review. *Frontiers in Materials* 7: 608139.

104 Chen, Y., Zhang, C., and Chen, P. (2021). Surface graft modification of domestic PBO fiber by atmospheric air plasma. *Chinese Journal of Materials Research* 35 (9): 641–650.

105 Chen, F., Zhang, M., Chen, L. et al. (2020). Anti-ultraviolet aging property and functionality enhancement of poly(p-phenylene benzobisoxazole) fiber coated with polydopamine. *Polymer Materials Science & Engineering* 36 (5): 153–160.

106 Liu, Z., Chen, B., and Chen, P. (2020). Treatment of oxygen dielectric barrier discharge plasma on PBO fiber surface and influence on its BMI composites. *Chinese Journal of Materials Research* 34 (2): 109–117.

107 Zeng, J., Kong, H., Du, X. et al. (2021). Surface modification of PBO fibers with 2,2-Bis (3-amino-4-hydroxyphenyl) hexafluoropropane in supercritical carbon dioxide for enhancing interfacial strength. *Materials Today Chemistry* 20: 100426.

108 Zheng, L.H., Yuan, L., Liang, G.Z., and Gu, A.J. (2019). An in situ (K0.5Na0.5)NbO3-doped barium titanate foam framework and its cyanate ester

resin composites with temperature-stable dielectric properties and low dielectric loss. *Materials Chemistry Frontiers* 3 (4): 726–736.

109 Wen, Y., Meng, X., Fan, W. et al. (2019). Study on polyimide fiber reinforced resin matrix composites. *New Chemical Materials* 47 (1): 57–61.

110 Yuan, Y., Diao, S., Zhao, C.D. et al. (2020). Preparation of hollow glass microsphere/organic silicone resin composite material with low dielectric constant by in-situ polymerization. *Silicon* 12 (6): 1417–1423.

111 Li, W.C., Huang, W., Kang, Y. et al. (2019). Fabrication and investigations of G-POSS/cyanate ester resin composites reinforced by silane-treated silica fibers. *Composites Science and Technology* 173: 7–14.

112 Meinders, R., Murphy, D., Taylor, G. et al. (2021). Development of fiber-reinforced transparent composites. *Polymers & Polymer Composites* 29 (9): S826–S834.

113 Liao, L., Peng, Z., Zhang, M., and Ruan, W. (2021). Research progress of low dielectric polymers for high-frequency printed circuit boards. *Journal of Functional Polymers* 34 (4): 320–335.

114 Martin, S.J., Godschalx, J.P., Mills, M.E. et al. (2000). Development of a low-dielectric-constant polymer for the fabrication of integrated circuit interconnect. *Advanced Materials* 12 (23): 1769–1778.

115 Wang, L., Yang, J., Cheng, W.H. et al. (2021). Progress on polymer composites with low dielectric constant and low dielectric loss for high-frequency signal transmission. *Frontiers in Materials* 8: 774843.

116 Huan, X., Shi, K., Yan, J. et al. (2020). High performance epoxy composites prepared using recycled short carbon fiber with enhanced dispersibility and interfacial bonding through polydopamine surface-modification. *Composites Part B: Engineering* 193: 107987.

117 Meireman, T., Daelemans, L., Rijckaert, S. et al. (2020). Delamination resistant composites by interleaving bio-based long-chain polyamide nanofibers through optimal control of fiber diameter and fiber morphology. *Composites Science and Technology* 193: 108126.

118 Qi, Q., Zheng, P., Lei, Y., and Liu, X. (2019). Design of bi-modal pore structure polyarylene ether nitrile/SiO2 foams with ultralow-k dielectric and wave transparent properties by supercritical carbon dioxide. *Composites Part B: Engineering* 173: 106915.

119 Yin, X.W., Cheng, L.F., Zhang, L.T. et al. (2017). Fibre-reinforced multifunctional SiC matrix composite materials. *International Materials Review* 62 (3): 117–172.

120 Zhang, C.L., Ye, F., Cheng, L.F. et al. (2021). Electromagnetic wave-transparent porous silicon nitride ceramic prepared by gel-casting combined with in-situ nitridation reaction. *Journal of the European Ceramic Society* 41 (15): 7620–7629.

121 Zhang, N.X., Jiang, H., Bai, M. et al. (2018). An exploration of finite frequency selective surface fringe effect to wave-transparent mechanism. In: *2018 International Applied Computational Electromagnetics Society Symposium in China (ACES-CHINA 2018)*.

122 Yin, J., Ma, W., Gao, Z. et al. (2022). An electromagnetic wave-transparent model based on plain fabric structural features. *Textile Research Journal* (8): 00405175221123064.

123 Yuan, H., Meng, Q., Zhang, H. et al. (2021). Preparation and properties of novel silicon-containing polyarylacetylene resin based wave-transparent composite. *Acta Materiae Compositae Sinica* 38 (11): 3629–3639.

124 Zhang, T., Sun, S., Cai, J.Q. et al. (2020). A new precursor to lightweight porous Si-Al-O-B ceramics with enhanced microwave transmissivity. *Ceramics International* 46 (2): 1974–1981.

125 Jiang, W.X., Zhang, X.H., Chen, D. et al. (2021). High performance low-k and wave-transparent cyanate ester resins modified with a novel bismaleimide hollow polymer microsphere. *Composites Part B: Engineering* 222: 109041.

126 Zhang, L., Mao, J.L., Wang, S. et al. (2019). Benzoxazine based high performance materials with low dielectric constant: a review. *Current Organic Chemistry* 23 (7): 809–822.

127 Jianjun, Y., Wensuo, M., Zuobin, G. et al. (2022). Electromagnetic wave-transparent model for 2D woven composites ellipsoid radome. *Mechanics of Advanced Materials and Structures* 77: 1–7.

128 Li, X.T., Zhu, X.M., Dong, J. et al. (2021). Preparation of low-dielectric permittivity polyimide resins with high surface activity from chemically bonded hyperbranched polysiloxane. *Chinese Journal of Polymer Science* 39 (9): 1200–1210.

129 Zu, Y., Zhang, F., Chen, D. et al. (2020). Wave-transparent composites based on phthalonitrile resins with commendable thermal properties and dielectric performance. *Polymer* 198: 122490.

130 Qu, C.Y., Chang, J.Y., Liu, C.W. et al. (2020). Novel allyl and propenyl monomers for modification of the bismaleimide resins, with excellent dielectric properties and high glass transition temperatures. *High Performance Polymers* 32 (1): 116–126.

131 MacDonald, M.E. (2019). An overview of radomes for large ground-based antennas. *IEEE Aerospace and Electronic Systems Magazine* 34 (10): 36–43.

132 Martellosio, A., Pasian, M., Perregrini, L. et al. (2017). High-frequency radomes for polar region ground stations: the state of the art and novel developments of radome technologies. *IEEE Antennas and Propagation Magazine* 59 (6): 88–101.

133 Qamar, Z., Aboserwal, N., and Salazar-Cerreno, J.L. (2020). An accurate method for designing, characterizing, and testing a multi-layer radome for mm-wave applications. *IEEE Access* 8: 23041–23053.

134 Xu, W.Y., Duan, B.Y., Li, P., and Qiu, Y.Y. (2017). Study on the electromagnetic performance of inhomogeneous radomes for airborne applications-part II: the overall comparison with variable thickness radomes. *IEEE Transactions on Antennas and Propagation* 65 (6): 3175–3183.

135 Liu, R.B., Han, Z.W., Li, W.F. et al. (2016). Improvement of the interfacial shear strength of poly(p-phenylene benzobisoxazole) fiber/epoxy resin composite via a novel surface coating agent. *Polymer Composites* 37 (4): 1198–1205.

136 Zimmermann-Ptacek, J., Muggli, M., Wildhack, S. et al. (2018). Thermal, dielectric, and mechanical properties of h-BN-filled PTFE composites. *Journal of Applied Polymer Science* 135 (44): 46859.

137 Wang, Y.Q., Zeng, Z., Gao, M., and Huang, Z.Y. (2021). Hygrothermal aging characteristics of silicone-modified aging-resistant epoxy resin insulating material. *Polymers* 13 (13): 2145.

138 Zou, C.R., Li, B., Liu, K. et al. (2019). Mechanical properties and interfacial characteristics of 2.5D SiNOf/BN wave-transparent composites. *Journal of the European Ceramic Society* 39 (10): 3013–3022.

139 Yang, B., Mao, Y.Y., Zhang, Y.H. et al. (2019). Fast-curing halogen-free flame-retardant epoxy resins and their application in glass fiber-reinforced composites. *Textile Research Journal* 89 (18): 3700–3707.